Geometry, kinematics and age of the northern half of the White Mountain shear zone, eastern California and Nevada

Walter A. Sullivan

Thesis submitted to the Faculty of Virginia Polytechnic Institute and State University in partial fulfillment of the requirements for the degree of

Master of Science

in

Geological Sciences

Committee
Richard D. Law, Chair
James A. Spotila
Robert J. Tracy

June 6, 2003

Blacksburg, VA

Keywords: shear zone, White Mountains, transpression, kinematic framework

Geometry, kinematics and age of the northern half of the White Mountain shear zone, eastern California and Nevada

Walter A. Sullivan

ABSTRACT

The White Mountain shear zone (WMSZ) is a zone of intense penetrative deformation that lies along the western front of the northern White-Inyo Range in eastern-most California and western-most Nevada. The northern half of the WMSZ is characterized by a NNE to NNW-striking steeply dipping foliation and associated shallowly plunging NNE to NW-trending stretching lineations. S-C fabrics observed in outcrop, microstructural shear sense indicators and kilometer-scale foliation geometry all indicate dextral movement.

Localized discrete zones of coeval steeply plunging stretching lineations are present in the northern half of the WMSZ. Microstructural data from these domains indicate a high component of pure shear within a separate coeval kinematic framework and hence a transpressional history. The WMSZ appears to be tectonically related to both the Sierra Crest shear system to the west and the Santa Rita shear system to the south. Correlation between the WMSZ and the Santa Rita shear system indicates that Late Cretaceous dextral transpression may extend up to ~120 km along the western front of the White-Inyo Range.

Cross-cutting relationships with Late Cretaceous plutons bracket the age of the WMSZ at between 72-92 Ma. A lack of annealing recrystallization in deformed quartz and the presence of high temperature crystallographic fabrics near the margins of the ca. 72 Ma Boundary Peak pluton indicate significant strain accumulation within the WMSZ subsequent to emplacement of the Boundary Peak pluton. These observations extend the duration of Late Cretaceous dextral transpression in eastern California to at least as recent as 72 Ma.

ACKNOWLEDGEMENTS

Grants

This project was partially funded by grants from the University of California San Diego White Mountain Research Station, the David R. Wones Geoscience scholarship fund and the Sigma Xi scientific society.

Personal

I would like to thank my family, especially my parents, for continually supporting me throughout my academic endeavors. I would not have made it this far without their examples or the lessons they have given me. Stephen Starcher has been instrumental in reminding me not to let my school work interfere with my education (a lesson learned from his father). Tim Schlack has been instrumental in reminding me of the value of an education outside of geology. Field work would not have been the same without those I came to know while staying at the White Mountain Research Station during the summer of 2002. All of the obstacles faced in completing this work were made smoother by my friends and colleagues in the Geology Department here at Virginia Tech, especially Jamie Buscher and Mariano Velazquez, and some other life long friends who, I am sure, know who they are. I am grateful to Jim Spotila and Bob Tracy for thoughtful reviews of my manuscript. Finally, I would like to thank my adviser, Rick Law. He has simultaneously allowed me freedom to think and act for myself while supporting me with answers and dialog whenever I felt the need. I consider myself privileged to have worked with him and would jump at the chance to do so again in the future.

DEDICATION

This work is dedicated to Donald S. Starcher and Douglas H. Jett who were called elsewhere before they could see its completion

TABLE OF CONTENTS

TABLE OF FIGURES

LIST OF TABLES

INTRODUCTION

Geologic structures exposed in eastern most California and western most Nevada record a complex deformational history beginning with the Carboniferous Antler Orogeny (Stevens et al. 1997 and references therein) and continuing to recent and ongoing strike-slip deformation (e.g., Reheis and Dixon, 1996; Reheis and Sawyer, 1997). During the Mesozoic, subduction along the western margin of North America was associated with formation of a continental magmatic arc, the Sierra Nevada Batholith, in addition to compressional and transpressional structures found both along the axis of the magmatic arc and behind the arc further inboard of the continental margin (Greene and Schweickert, 1995; Stevens et al. 1997 and references therein; Tikoff and Greene, 1997; Tikoff and Saint Blanquat, 1997).

The White-Inyo Range is the western most crustal block in the central Basin and Range Province, and is situated on the inboard margin of the Sierran magmatic arc (Fig. 1). This paper is concerned with a zone of intense penetrative deformation of apparent Mesozoic age, the White Mountain shear zone (WMSZ), which is exposed along the western front of the northern White Mountains in California and Nevada (Figs. 1, 2). The regional extent of the WMSZ was demarcated by U.S.G.S. quadrangle mapping (Crowder et al., 1972; Crowder and Sheridan, 1972), and the WMSZ has previously been interpreted to be a thrust fault (Crowder and Sheridan, 1972; Dunne et al., 1983), a strike-slip fault (Schweikert, 1981), or a suture zone between terrains (Nokleberg, 1983). Most recently, based on observations made near the southern end of the WMSZ, Hanson (1986, 1987) proposed two episodes of deformation; Jurassic east-directed thrusting and Cretaceous dextral strike-slip movement. All of these interpretations, however, are based on reconnaissance level structural data, and little or no structural data has been available for most of the northern half of the WMSZ. Consequently, this paper presents and integrates detailed field and petrographic data from the northern half of the WMSZ in order to generate a more comprehensive understanding of the geometry, kinematics and timing of deformation within the WMSZ and its tectonic significance with respect to other Mesozoic structures in the region.

GEOLOGIC SETTING

Northern White-Inyos

Two Late Cretaceous plutons, the Pellisier Flats pluton and the Boundary Peak pluton, dominate the bedrock geology of the northern White Mountains, with the Boundary Peak pluton being hosted almost entirely within the Pellisier Flats pluton (Fig. 2) (Crowder et al., 1972). The Pellisier Flats pluton has been dated at 91.7 +/- 0.7 Ma ($^{40}Ar/^{39}Ar$) and 88.0 +/- 2.7 Ma (K-Ar) by McKee and Conrad (1996), 89.6 Ma (U-Pb) by Stern et al. (1981) and 92.3 +/- 3.0 Ma (U-Pb) by Crowder et al. (1973). The Boundary Peak pluton has been dated at 71.7 +/- 0.7 Ma ($^{40}Ar/^{39}Ar$) and 72.9 +/- 2.5 Ma (K-Ar) by McKee and Conrad (1996) and 73.7 +/- 2.2 Ma (U-Pb) by Crowder et al. (1973). Locally, marble and lesser amounts of schist and quartzite of probable Paleozoic protolith age are exposed along the margins of the Late Cretaceous plutons and as xenoliths hosted within the plutons. South and east of the Pellisier Flats pluton there are extensive exposures of Mesozoic metavolcanic and metasedimentary rocks (Fig. 2) (Crowder and Sheridan, 1972). An ash-flow tuff from the metavolcanic section has yielded an U-Pb age of 152 +5/-1 Ma (Hanson, 1986).

As noted above, the regional extent of the WMSZ was demarcated by U.S.G.S. quadrangle mapping in the 1960's and 1970's. In the north, the WMSZ primarily deforms the ca. 92 Ma Pellisier Flats pluton and the marbles and schists lying along the western front of the range (Crowder et al., 1972). Near the southern end of the zone, the deformation fabric cuts the Mesozoic metavolcanic and metasedimentary units (Crowder and Sheridan, 1972). Crowder et al. (1972) recognized a weak fabric within parts of the ca. 72 Ma Boundary Peak pluton, and, based on this, proposed a Late Cretaceous age for at least the most recent movement along the shear zone.

In addition to Cenozoic normal faulting associated with Basin and Range extension, Hanson (1986) recognized three distinct fabrics (D-1, D-2 and D-3) within the Mesozoic rocks of the northern White Mountains near the southern terminus of the mapped extent of the WMSZ. Hanson's D-1 fabric is characterized by a ~N-S-striking foliation, a shallowly to steeply plunging SW-trending lineation and small tight to isoclinal folds with axial planes roughly parallel to the D-1 foliation. This D-1 fabric is best developed within the WMSZ, but not observed in the Pellisier Flats pluton. Hanson's D-

2 fabric is characterized by N-S-trending west-vergent folds and thrust faults that apparently deform D-1 fabrics outside of the WMSZ, but are poorly developed within, or structurally isolated from, the WMSZ. Finally, Hanson's D-3 fabric is characterized by E-W-trending crenulation, kink and/or large broad folds that are recognized throughout the Mesozoic metavolcanic/metasedimentary section. Additionally, Hanson (1986, 1987) recorded a N-S-striking foliation and a shallowly plunging N-S-trending lineation that is best developed within the WMSZ and is associated with dextral S-C structures observed in the Marble Creek area. Based on these observations from the extreme southern end of the WMSZ, Hanson (1986, 1987) proposed two episodes of deformation for the WMSZ: 1) east-directed reverse faulting associated with the D-1 fabric, and 2) N-S-oriented dextral strike-slip movement associated with the apparently younger D-3 fabric and postdating emplacement of the Pellisier Flats pluton.

Cenozoic extensional faulting

It is widely recognized that many areas within the Basin and Range Province, including the White-Inyo Range, are characterized by individual ranges consisting of relatively intact footwall blocks, bounded on one side by range-scale high angle normal fault systems that exhibit tilting due to normal fault offset (e.g., Stewart, 1980). Much of the White-Inyo Range is bounded on the west by the steeply west-dipping White Mountains fault zone which accommodates as much as 8-9 km of normal displacement (Stockli et al., 2000, in press). Detailed mapping of Oligocene and Early Miocene volcanic and volcaniclastic rocks deposited unconformably on Mesozoic and older plutonic and metamorphic rocks along the eastern margin of the White-Inyo Range indicates that faulting associated with Basin and Range tectonism has rotated the northern part of the range ~25° clockwise (i.e. down to the east) about a horizontal axis trending ~355° (Stockli et al., in press).

DATA COLLECTION

This study was largely limited to the northern half of the WMSZ for three reasons. First, as mentioned above, Hanson (1986, 1987) has provided some structural data for the southern end of the shear zone, but little or no structural data was available for most of the northern half of the WMSZ. Second, the lithologic relationships in the northern half of the shear zone are simpler making structural variations easier to recognize. Finally,

detailed study of overprinting relationships between deformation fabrics and the margins of the Late Cretaceous plutons provided an opportunity to better constrain the age of the WMSZ.

Due to the size of the area (~21.5 x 2 km) and the rugged nature of the topography, detailed field mapping of the northern half of the WMSZ is impractical. Consequently, field data was collected along 8 detailed traverses oriented at near right angles to the shear zone margins. Emphasis was placed on mapping orientation of foliation and lineation within the mylonitic fabric, and on documenting variations in fabric intensity. Particular attention was also given to cross-cutting relationships with the Late Cretaceous plutons in order to better constrain the timing of deformation. Close to 100 oriented samples were collected during field mapping, and 50 oriented thin sections cut perpendicular to foliation and parallel to the mineral lineation were prepared from the samples for kinematic analyses. Seven of these thin sections contained quartz domains suitable for the optical measurement of quartz c-axis fabrics using the universal stage.

In order to attempt to correct for tilting associated with Basin and Range extension, all of the structural orientation data presented in this paper has been rotated 25° counterclockwise (i.e. down to the west) about a horizontal axis trending towards 355° (c.f. Stockli et al., in press). A complete listing of all unrotated and rotated orientation data collected for this study is presented in Tables 2 and 3 in Appendix A.

SHEAR ZONE GEOMETRY

The orientation data described below have been rotated as discussed above so that any tectonic interpretations of the data are based on orientations that predate Basin and Range tilting. At its northern end, in the Morris Creek area, the WMSZ is represented by a NE to NNE-striking foliation. The rocks exhibiting the highest finite strain in this area are located along the range front. Moving eastward, towards the shear zone margins the strike of the foliation progressively changes from ~035° in the high strain rocks to ~020-015° closer to the shear zone margins. The dip of foliation also changes from vertical near the range front to steep-to-the-W closer to the shear zone margins. Stretching lineations near the northern end of the WMSZ trend N to NNE and are shallowly to moderately plunging (Figs. 2, 3, 4).

Just to the south of the Morris Creek area, the dip of foliation becomes locally more variable, varying between steep and shallow dips to both the E and W (Fig. 5). In this area zones of steeply plunging NNE-trending stretching lineations have also been recognized (Fig. 5). These domains of steep stretching lineations are normally laterally very restricted and can occasionally be traced into zones of shallowly plunging lineations within a single outcrop (Figs. 2, 5).

To the south, between Morris and Marble creeks the strike of foliation in the highest strain rocks gradually swings from NE to NNE to N-S, and the dip of foliation remains consistently near-vertical to steep-to-the-W with some areas of steep-to-the-E dip found near the range front (Map 1). The trend of stretching lineations swings from NNE to N, and the plunge remains shallow to moderate. Domains of steeply plunging stretching lineations were recognized in the Montgomery Canyon area and just to the south (Map 1).

In the Marble Creek area (Figs. 6, 8), foliation within the WMSZ strikes NNE to NNW near the range front, where the highest-strain fabrics are found, and swings to the NW to WNW near the margins of the shear zone to the east. Moving eastward, the dip of foliation changes from steep-to-the-E at the range front to near-vertical to steep-to-the-W as the strike of foliation swings around to the NW and the deformation fabric weakens. Stretching lineations in the Marble Creek area trend towards the N to NW and are shallowly plunging (Figs. 2, 3, 6). Steeply plunging stretching lineations were not observed in the Marble Creek area.

At the southern end of the study area, near Falls Canyon (Figs. 7, 8), the WMSZ is characterized by a NW to NNW-striking steeply W-dipping to near-vertical foliation associated with NNW-trending shallowly to moderately plunging stretching lineations. Localized domains of steeply plunging stretching lineations, similar to those described just to the south of Morris Creek, are present in outcrops near the range front (Figs. 2, 3, 7). Additionally, in the Falls Canyon area, the highest finite strains are found in the marbles, schists and quartzites located along the range front, whereas finite strain within the Pellisier flats pluton is generally lower and quite heterogeneous with some locations within the shear zone having no observable fabric.

Between Marble Creek and Falls Canyon (Fig. 8A), in the central part of the WMSZ, there is a broad zone of consistently NW to WNW-striking, near-vertical to steeply W-dipping foliation, characterized by relatively low finite strains. In this area, the deformation fabric steps roughly 2 km to the east in plan view before the strike of foliation swings back to a more N-S orientation near Falls Canyon (Figs. 2, 3, 8). Reconnaissance-level data collected during this study and data collected by Hanson (1986) indicate that south of the study area foliation within the WMSZ continues to strike to the NNW. It is proposed that the broad zone of NW to WNW-striking foliation between Marble Creek and Falls Canyon represents a left-stepping transfer zone between discrete NNE and NNW-striking segments of the ~N-S-trending WMSZ that allows for an E-W step of the main deformation zone of roughly 2 km (Fig. 8B).

Finally, the northern segment of the WMSZ is somewhat arcuate in shape, with the deformation fabric between Marble Creek and the northern end of the shear zone being bowed out to the west (Fig. 3). By comparison, the southern segment of the WMSZ within the study area appears to be fairly linear. Some possible implications of this geometry will be discussed below.

KINEMATICS

Kinematic framework

As discussed above, the northern half of the WMSZ is characterized by a NNE to NNW-striking near-vertical to steeply W-dipping foliation and associated NNE to NW-trending gently to moderately plunging stretching lineations. This geometry is consistent with that expected for a ~N-S-trending strike-slip shear zone. Interspersed within this general framework are discrete domains of steeply plunging N to NW-trending stretching lineations that in some cases grade successively into domains of shallowly plunging lineations within a single outcrop. Such domains of steeply plunging lineations were observed in both the Pellisier Flats pluton and in the Paleozoic marbles, schists and quartzites along the western front of the range.

Shear sense

All shear sense indicators discussed here were observed on section planes oriented perpendicular to the main foliation and parallel to the stretching lineation. Hence, in the

zones exhibiting a steeply dipping foliation and sub-horizontal stretching lineations, the section planes are viewed looking vertically down into the ground. S-C fabrics indicating a dextral shear sense (Berthe et al., 1979) are often well developed within the Pellisier Flats pluton and are commonly observed in outcrop within the northern half of the WMSZ (Fig. 3; Map 1). C-surfaces are typically defined by planar domains of biotite, chlorite and quartz ribbons while S-surfaces are typically defined by alignment of elongate feldspar porphyroclasts separated by biotite, chlorite and quartz ribbons. The most spectacular examples of S-C fabrics are found at the extreme northern end of the shear zone in a coarse grained facies of the Pellisier Flats pluton exposed in the Morris Creek area where individual C-surfaces are separated by as much as 2 cm (Fig. 9-A).

Shear sense indicators observed in thin-section from sub-horizontally lineated samples are almost universally dextral and most commonly include type-I and type-II S-C fabrics (Lister and Snoke, 1984) and C′ structures (Hanmer and Passchier, 1991). Within type-II S-C fabrics, C-surfaces are defined by an alignment of biotite, chlorite and opaque minerals (Fig 9-B). Asymmetric quartz c-axis fabrics also confirming a dextral shear sense have been recorded from just north of the Morris Creek area and from the Marble Creek area (Fig. 10-A, B, E).

An overall dextral shear sense for the WMSZ is also indicated by the kilometer-scale foliation geometry. In the Marble Creek area, the strike of foliation swings from ~N-S in the high strain rocks near the range front to ~NW near the shear zone margins (Figs. 3, 6). Such a swing in the strike of foliation is very similar to that expected for half of an ideal dextral strike-slip simple shear zone (c.f. Fig. 8B) (Ramsay and Graham, 1970). This feature is also present in the Morris Creek area where the strike of foliation swings ~15-20° to the west between the high strain rocks located along the range front and the eastern margin of the shear zone (Figs. 3, 4). Thus, it appears that along much of its length the northern half of the WMSZ has been cut in half along its length by Cenozoic normal faults, leaving only the eastern half of a dextral strike-slip shear system exposed (Fig. 3).

Steeply plunging lineations

As discussed above, domains of steeply plunging lineations can be observed in several locations within the northern half of the WMSZ. In some cases, these domains grade

successively into typical shallowly lineated mylonites within a single outcrop and domains of steeply plunging stretching lineations are found within domains exhibiting both relatively high and low finite strain. These two factors indicate that the steeply plunging and shallowly plunging stretching lineations observed in the northern half of the WMSZ are cotemporaneous.

Microstructure-based kinematic data collected from domains within the WMSZ exhibiting stretching lineations with a rake of more than 45° are summarized in Table 1.

Sample Location	Orientation of Foliation	Orientation of Lineation	Rake of Lineation	Microstructure based shear sense indication	Motion	Direction	Quartz C-axis fabric	Relative finite strain	Lithology
161	329/62-E	013-52	64	None	Pure shear	N/A	Not measurable	Low	Pelisier Flats
174	050/61-N	023-40	48	None	Pure shear	N/A	Not measurable	High	Pelisier Flats
177	021/75-W	358-54	58	Weak shear bands	Reverse	Top up to east	Not measurable	Low	Pelisier Flats
064	350/75-W	292-73	81	None	Pure shear	N/A	Not measurable	Medium	Pelisier Flats
065	009/72-W	347-51	54	Weak type II S-C	Normal	Top down to west	Symmetric X-girdle	High	Quartzite/ Schist
069	003/68-W	340-40	49	None	Pure shear	N/A	Symmetric X-girdle	High	Quartzite/ Marble
156	310/84-E	318-61	62	Shear bands	Reverse	Top up to west	Not measurable	Medium	Pelisier Flats
135	317/79-E	112-49	53	None	Pure shear	N/A	Not measurable	High	Marble
137	336/68-W	316-42	45	Type II S-C	Normal	Top down to west	Symmetric X-girdle	Medium	Quartzite/ Schist

Table 1: Table summarizing sample orientations and kinematic data collected from oriented thin sections where the rake of the stretching lineation in the foliation was greater than 45°.

Of the nine samples for which this data is available, five exhibit no discernable sense of fabric asymmetry. These five samples span the range of relative finite strains observed in the steeply lineated domains, and the lack of fabric asymmetry is attributed to a high component of pure shear. In geographic coordinates, two of the remaining samples yielded a top-down-to-the-west normal motion, one yielded a top-up-to-the-east reverse motion and one yielded a top-up-to-the-west reverse motion. In other words, no consistent sense of motion was observed in the steeply lineated domains. Nearly symmetrical cross-girdle quartz c-axis fabrics were collected from two of the high strain

samples and one of the medium strain samples, and the presence of these fabrics supports the notion that the steeply lineated zones contain a high component of pure shear (Law, 1990 and references therein). Based on these observations, it appears that within the northern half of the WMSZ there are localized discrete zones containing a relatively high component of pure shear, and, as a result, a transpressional deformational history will be proposed below.

TIMING OF DEFORMATION

Field relations

As mentioned above, Crowder et al. (1972) recognized that within the WMSZ the ca. 92 Ma Pellisier Flats pluton is intensely deformed, whereas only a weak deformational fabric exists within parts of the ca. 72 Ma Boundary Peak pluton. Fabrics within the Boundary Peak pluton are best developed in the Morris Creek area (Fig. 4) and generally consist of a weak foliation defined by local stretched quartz and an alignment of biotite grains. The orientation of foliation within the Boundary Peak pluton is consistent with that from the rest of the WMSZ. Sheared dikes of the Boundary Peak pluton were observed from Morris Creek south to the Marble Creek area. These observations roughly bracket the age of the WMSZ between 92 and 72 Ma.

Single deformational episode

Deformation within the northern half of the WMSZ that predates the emplacement of the Pellisier Flats pluton seems unlikely for two reasons. First, quartz from quartzite and schist units found near the margins of the Pellisier Flats pluton in Falls Canyon (Fig. 7) has undergone relatively low temperature regime-II dynamic recrystallization (i.e. subgrain rotation recrystallization; Hirth and Tullis, 1992) and exhibits little or no annealing recrystallization (Fig. 9-B). This indicates that the quartz was deformed well after any contact metamorphism associated with emplacement of the Pellisier Flats pluton. Second, in the northern half of the WMSZ domains of steeply plunging stretching lineations have been recognized both in the Pellisier Flats pluton and in the surrounding Paleozoic age metamorphic rocks, and evidence presented in this paper shows them to be coeval with shallowly plunging lineations. It may be that the steeply plunging lineations recognized by Hanson (1986, 1987) in the southern part of the WMSZ do

indeed represent an earlier deformational episode. Unfortunately, with only reconnaissance-level field data available south of Falls Canyon, it is impossible to determine the relative ages of steeply plunging lineations near the southern end of the shear zone. Consequently, the interpretation of a single Late Cretaceous episode of deformation for the WMSZ will only be extended to the field area of this study.

TEMPERATURE OF DEFORMATION

From Marble Creek south, quartz deformation is dominated by regime-II (subgrain rotation) recrystallization as defined by Hirth and Tullis (1992) (Figs. 9-B, 9-C). Deformation temperatures estimated from the opening angles of quartz c-axis fabrics (Kruhl, 1998) within samples collected from Marble Creek and Falls Canyon are consistently in the 400-450 °C range (Figs. 10-12). Moving north towards the margins of the Boundary Peak pluton, quartz deformation changes to a mixture of regime-II and III (grain boundary migration) recrystallization in the Pellisier Flats pluton and is well into regime-III in quartz-rich metasedimentary xenoliths. Additionally, these samples appear to have undergone little or no annealing recrystallization (Figs. 9-D, 9-E). Within the Pellisier Flats pluton, regime-II quartz recrystallization is largely localized in the high strain shear bands and C-surfaces (Fig. 9-D). Hence, it appears that, in these samples, the transition between regime-II and III recrystallization is being controlled by heterogeneities in strain rate, because the mm-scale variations in recrystallization mechanisms cannot be explained by temperature variations. Temperatures estimated from the opening angles of crystallographic fabrics collected from samples from near the margins of the Boundary Peak pluton are in the 500-575 °C range (Figs. 10-12). One of these samples, 188, is characterized by a mixture of strain rate-controlled regime-II & III recrystallization as described above. Opening angles of quartz c-axis fabrics are controlled by the slip systems active during deformation, and the activation of slip systems is in turn controlled by a combination of temperature, strain rate and fluid activity (Law, 1990 and references therein). Higher opening angles are favored by high temperatures, slow strain rates and high fluid activities (Tullis et al., 1973). Consequently, the temperature estimate for sample-188 may be lower than the actual temperature of deformation due to the localized relatively high strain rates experienced in the quartz domains.

To summarize, temperatures similar to those expected for greenschist facies conditions were present during deformation in the southern part of the study area between Falls Canyon and Marble Creek. At the same time, near the Boundary Peak pluton at the northern end of the shear zone, temperatures similar to those expected for upper greenschist to epidote-amphibolite facies conditions were present. In other words, there appears to be a 100 °C difference in the temperature of deformation over a horizontal distance of 11 km or less between the Falls Canyon area and the southern end of the Boundary Peak pluton. Furthermore, quartz in samples collected from within 400 m of the margins of the Boundary Peak pluton has undergone little or no annealing recrystallization, indicating that deformation continued after emplacement of the Boundary Peak pluton.

DISCUSSION

Field and petrographic data presented in this study demonstrate that the northern half of the WMSZ represents a N-S-trending dextral transpressional shear system of Late Cretaceous age. Moreover, field, microstructural and crystallographic fabric data from the WMSZ indicate that deformation continued after emplacement of the Boundary Peak pluton at ca. 72 Ma. Although there is no direct evidence for deformation predating emplacement of the Pellisier Flats pluton in the northern half of the WMSZ, data presented in this study cannot rule out the existence of earlier deformational episodes in the southern end of the WMSZ as outlined by Hanson (1986, 1987).

Timing constraints based on quartz deformation

There are two ways to explain the observed temperature variations between the northern end of the WMSZ and the Falls Canyon area: 1) there has been significantly more exhumation in the northern part of the study area, exposing deeper levels of the crust, or 2) deformation along the WMSZ continued for at least a short time subsequent to heating caused by the emplacement of the Boundary Peak pluton. Evidence presented by Stockli (in press) indicates that over a horizontal distance of ~26 km between the northern and central White Mountains, there is only a 2 km difference in normal fault offset along the front of the range. These observations make it seem unlikely that differences in the amount of exhumation due to Cenozoic extensional faulting associated with Basin and Range tectonism can explain the observed

temperature variations. The evidence presented by Stockli et al. (in press) does not rule out a significant amount of differential exhumation predating Cenozoic faulting. However, there does not appear to be a structural mechanism allowing for significantly greater amounts of exhumation in the northern part of the study area between the cessation of movement along the WMSZ and the onset of Cenozoic extensional faulting. Regional greenschist facies grade metamorphism within the central White-Inyos is Jurassic or older in age, and no Late Cretaceous metamorphism has been recognized outside of contact areoles surrounding intrusive bodies (Morgan and Law, 1998). These observations indicate that the high deformation temperatures of Late Cretaceous age found within the northern half of the WMSZ were caused by localized magmatic heating rather than regional scale metamorphism. Thus, the observed variations in quartz deformation temperatures between the northern and southern halves of the WMSZ were most likely caused by heating associated with emplacement of the Boundary Peak pluton.

Numerical simulations of quartz fabric development indicate that, in quartzites, shortening on the order of 40% is needed to cause gross changes to a pre-existing fabric (Hobbs, 1985). Based on this, the existence of well developed high temperature crystallographic fabrics in steeply lineated sheared quartzite xenoliths (Figs. 10, 11; and Table 1) from near the margins of the Boundary Peak pluton indicates that a significant amount of strain must have accumulated after the emplacement of the pluton and subsequent magmatic heating of the surrounding country rocks.

Arcuate shape of the northern segment of the WMSZ

As noted under the section headed “shear zone geometry”, the northern segment of the WMSZ is arcuate in shape, and appears to be bowed outwards to the west (Fig. 3). At first glance, it might appear that such a westward bowing of the WMSZ may be due to bulging associated with forceful emplacement of the Boundary Peak pluton similar to that described for the Papoose Flat pluton in the southern White-Inyo Range (e.g. Law et al., 1992; Morgan et al., 1998; Saint Blanquat et al., 2001). If the arcuate shape of the northern segment of the WMSZ were indeed due to forceful emplacement of the Boundary Peak pluton, then it would be plausible that the deformation fabrics observed in that area were partially or wholly a result of deformation associated with pluton emplacement rather than regional transpression. This seems unlikely for four reasons.

First, there is no evidence of forceful emplacement elsewhere around the margins of the Boundary Peak pluton. Second, the kinematic framework within the shallowly lineated domains is consistent throughout the field area of this study indicating that deformation fabrics throughout the shear zone formed in response to the same regional stress field. Third, the sense of motion within shallowly lineated domains remains constant throughout the northern half of the WMSZ indicating that the deformation fabric did not form in response to stretching around the margins of a forcefully emplaced pluton. Fourth, timing constraints based on quartz deformation discussed above indicate that a significant amount of deformation occurred after the emplacement of the Boundary Peak pluton. It may be that the arcuate nature of the northern segment of the WMSZ is due to bulging associated with the emplacement of the Boundary Peak pluton that occurred well before the cessation of movement along the shear zone. Another possible explanation is that strain was preferentially transferred into the belt of marble and schist lying along the western front of the range (Fig. 3), causing the WMSZ to follow a preexisting structural weakness. The latter hypothesis is supported by the preferential localization of strain into marble and schistose units in the Falls Canyon area as discussed above. However, it is difficult to draw any firm conclusions on the arcuate nature of the northern WMSZ with the data available.

Significance of steeply plunging lineations

Similar variations in the orientation of stretching lineations to those described here have been documented for the ca. 80-90 Ma dextral transpressional Sierra Crest shear system (SCSS) located along the axis of the Sierran magmatic arc to the west of the WMSZ (Fig. 1) (Greene and Schweickert, 1995; Tikoff and Greene, 1997; Tikoff and Saint Blanquat, 1997). Numerical models developed for the SCSS assume that the transition between steeply plunging and shallowly plunging stretching lineations occurs because, in homogeneous wrench-dominated transpression with a stable external kinematic framework, incremental strain from a vertical component of pure shear accumulates more efficiently than incremental strain from a larger horizontal component of simple shear. Initially, at relatively low finite strains, stretching lineations will be horizontal as expected for a transcurrent simple shear zone. At a certain level of finite strain, however, a switch in the finite stretch from horizontal to vertical will occur as the component of vertical pure shear becomes more important and material within the shear zone is extruded upwards towards the earth's surface. Consequently, assuming a

homogenous kinematic framework, the steeply plunging stretching lineations should be found in the areas of the shear zone with the highest finite strain (Tikoff and Greene, 1997; Tikoff and Saint Blanquat, 1997).

Two lines of evidence indicate that this model developed for the SCSS does not apply to the WMSZ. First, in the WMSZ, the zones of steeply plunging stretching lineations are found both in areas of relatively high finite strain and relatively low finite strain (Table 1). This observation indicates that the orientation of stretching lineations is independent of finite strain. Second, numerical simulations of quartz crystallographic fabric formation indicate that crystallographic fabric geometry and orientation is controlled by the external kinematic framework rather than by finite strain (e.g., Lister and Hobbs, 1980; Jessell and Lister, 1990). Consequently, in the models developed for the SCSS, crystallographic fabrics should be in the same orientation with respect to geographic coordinates for both steeply and shallowly lineated zones. This is not, however, the case in the WMSZ. C-axis fabrics from both shallowly and steeply lineated samples from the WMSZ measured in section planes cut perpendicular to foliation and parallel to lineation are all characterized by well developed girdles (single or cross) oriented at a high angle to the foliation plane and centered about the Y finite strain axis (Fig. 10). Thus, the orientation of crystallographic fabrics from the WMSZ indicates that the orientation of stretching lineations within these samples has remained constant with respect to the crystallographic fabrics and hence the external kinematic framework imposed upon the samples.

Based on the arguments presented above, it seems that the zones of steeply plunging stretching lineations found within the northern half of the WMSZ must represent a kinematic framework that localizes relatively large components of pure shear and is separate from, but coeval with, the dominate dextral transcurrent framework of the WMSZ discussed earlier. This assertion could be tested by conducting vorticity analyses on both the steeply lineated zones and on the typical shallowly lineated portions of the WMSZ. However, in most instances, the nature of the mylonites within the WMSZ makes them unsuitable for existing vorticity analysis techniques such as those discussed by Passchier (1988), Simpson and De Paor (1993, 1997) and Wallis (1992, 1995).

Segregated coeval domains of steeply and shallowly plunging stretching lineations have also been recognized in the dextral transpressional Santa Rita shear system (SRSS) exposed along the western front of the southern White-Inyo Range ~67 km south of the WMSZ (Fig. 1) (Vines 1999). The SRSS is entirely hosted within the ca. 164 Ma Santa Rita Flat pluton, and both steeply and shallowly lineated domains contain a steeply dipping NNW-striking foliation (Vines, 1999). Steeply lineated domains within the SRSS are laterally continuous and are oriented at roughly 45° to the overall trend of the shear zone, and shear sense indicators in these domains generally suggest a top-to-the-WSW reverse sense of motion (Vines 1999). White mica is absent in the Santa Rita Flat pluton, and syntectonic white mica separated from mylonites collected from the SRSS has yielded an Ar-Ar cooling age of 82-84 Ma indicating that the shear system was active at this time (Vines and Law, personal communication, 2002).

The conceptual kinematic model developed for the SRSS by Vines (1999) assumes that the principal stress direction present at the time of deformation was horizontal and oriented at an angle greater than 30° to the shear zone margins. Consequently, steeply lineated domains absorb a component of compression across the shear system through top-to-the-WSW reverse motion while dextral transcurrent motion is partitioned into the domains of shallowly plunging stretching lineations. The conceptual kinematic model for the WMSZ proposed above differs from Vines' (1999) model for the SRSS in two ways. First, in the WMSZ the compressional component is largely absorbed by penetrative pure shear. Moreover, in the steeply lineated zones where shear sense has been observed, there is no consistent sense of motion in geographic coordinates. Second, the compressional component within the WMSZ is localized into discrete laterally restricted zones with no consistent geometric relationship with the shear zone margins rather than the constantly oriented laterally continuous domains observed in the SRSS.

In summary, it seems that transpression within the WMSZ is related to that observed within the SCSS geometrically, temporally and in that the compressional component is primarily accommodated by pure shear. However, the two differ in that the WMSZ exhibits two separate kinematic frameworks with the pure shear-dominated extrusion largely taking place within discrete domains. Similarly, it seems that transpression within the WMSZ is related to that observed within the SRSS

geometrically, temporally and in that the compressional component is segregated from the transcurrent component of deformation. However, the two differ in that the compressional component within the SRSS is accommodated by top-to-the-WSW reverse motion rather than by pure shear. It would be interesting to compare the segregated kinematic framework models for the WMSZ and SRSS to the homogenous kinematic framework numerical model developed for the SCSS using quartz c-axis fabric orientation. However, in the absence of quartz c-axis fabric data from the SCSS, such a comparison is not possible.

Finally, based on the evidence presented in this paper, evidence for Late Cretaceous dextral transpression inboard of the SCSS can be extended ~100 km along strike northward from the SRSS along the western front of the White-Inyo Range, and can be extended in duration to as recent as 72 Ma. Moreover, it may be that the WMSZ and the SRSS represent the exposed remnants of a transpressional shear system similar in size to the SCSS, with the western portion of the shear system lying beneath the Owens Valley in the hanging wall block of the range front normal fault system.

Effects of Cretaceous transpression on Cenozoic extension

Previous workers have noted the close relationship between the location of the brittle Cenozoic White Mountains fault zone and the plastically deformed rocks of the WMSZ (Stockli et. al., in press and references therein). This relationship is especially strong in the extreme northern White-Inyo Range where the White Mountains fault zone cuts the Pellisier flats pluton, and is consolidated into a single large normal fault strand, with the trace of the fault being outlined by the western front of the range. Data presented in this paper show that the western front of the northern White Mountains roughly follows the strike of the vertical to steeply west-dipping foliation within the WMSZ (Fig. 3). Thus, the location of high angle Cenozoic normal faults within the White Mountains fault zone appears to not only have been influenced by the zone of weakness formed by the WMSZ, but to have also been directly controlled by the orientation of foliation within the WMSZ. In the southern White-Inyo Range, the orientation of foliation within the SRSS appears to have similarly controlled the geometry of NNW-striking range-bounding Cenozoic normal faults. Additionally, the WMSZ and SRSS mark the only locations where the range-bounding Cenozoic normal faults on the western flank of the White-Inyo Range have cut significant amounts of plutonic rock. Thus, it appears that these two

Late Cretaceous shear zones have strongly influenced the orientation and location of later Cenozoic normal faulting and hence the geomorphology of the White-Inyo Range.

REFERENCES

Berthe, D., Choukroune, P., and Gapais, D., 1979, Orthogneiss mylonite and noncoaxial deformation of granites: the example of ther South Armorican shear zone: Journal of Structural Geology, v. 1, p. 31-42.

Crowder, D.F., Robinson, P.F., and Harris, D.L., 1972, Geologic map of the Benton quadrangle Mono County, California and Esmeralda and Mineral Counties, Nevada: U. S. Geological Survey, scale 1:62,500, 1 sheet.

Crowder, D.F., and Sheridan, M.F., 1972, Geologic map of the White Mountain Peak quadrangle Mono County, California: U. S. Geological Survey, scale 1:62,500, 1 sheet.

Crowder, D.F., McKee, E.H., Ross, D.C., and Krauskopf, K.B., 1973, Granitic rocks of the White Mountains area, California-Nevada: age and regional significance: Geological Society of America Bulletin, v. 84, p. 285-296.

Dunne, G.C., Moore, S.C., Gulliver, R.M., and Fowler, J., 1983, East Sierran thrust system, eastern California: Geological Society of America Abstracts with Programs, v. 15, p. 322.

Greene, D.C. and Schweickert, R.A., 1995, The Gem Lake shear zone: Cretaceous dextral transpression in the Northern Ritter Range pendant, eastern Sierra Nevada, California: Tectonics, v. 14, no. 14, p. 945-961.

Hanmer, S. and Passchier, C.W., 1991, Shear-sense indicators: a review: Geological Survey of Canada, paper 90-17, 72 p.

Hanson, R.B., 1986, Geology of Mesozoic metavolcanic and metasedimentary rocks, northern White Mountains, California: Unpublished Ph. D. thesis, Los Angeles, University of California, 295 p.

Hanson, R.B., 1987, Sumperimposed deformations in the development of a shear zone: an example from the northern White Mountains, California: Geological Society of America Abstracts with Programs, v. 19, no. 7, p. 693.

Hirth, G. and Tullis, J., 1992, Dislocation creep regimes in quartz aggregates: Journal of Structural Geology, v. 14, p. 145-160.

Hobbs, B.E., 1985, The geological significance of microfabric analysis, *in* Wenk, H.R., ed., Preferred orientations in deformation metals and rocks: an introduction to modern texture analysis: Orlando, Academic Press, p. 463-484.

Jessell, M.W. and Lister, G.S., 1990, A simulation of the temperature dependence of quartz fabrics, *in* Knipe, R. J., and Rutter, E. H., eds., Deformation mechanisms, rheology and tectonics: Geological Society of London Special Publication, no. 54, p. 353-362.

Kruhl, J.H., 1998, Prism- and basal-plane parallel subgrain boundaries in quartz: a microstructural geothermobarometer: Reply: Journal of Metamorphic Geology, v. 16, p. 142-146.

Law, R.D., 1990, Crystallographic fabrics: a selective review of their applications to research in structural geology, *in* Knipe, R. J., and Rutter, E. H., eds., Deformation mechanisms, rheology and tectonics: Geological Society of London Special Publication, no. 54, p. 335-352.

Law, R.D., Morgan, S.S., Casey, M., Sylvester, A.G., Nyman, M., 1992, The Papoose Flat Pluton of eastern California; a reassessment of its emplacement history in the light of new microstructural and crystallographic fabric observations: Geological Society of America Special Paper, v. 272, p. 361-375.

Lister, G.S. and Hobbs, B.E., 1980, The simulation of fabric development during plastic deformation and its application to quartzite: the influence of deformation history. Journal of Structural Geology, v. 2, p. 355-370.

Lister, G.S., and Snoke, A.W., 1984, S-C mylonites: Journal of Structural Geology, v. 6, no. 6, p. 617-638.

McKee, E.H., and Conrad, J.E., 1996, A tale of 10 plutons, revisited: Age of granitic rocks in the White Mountains, California and Nevada: Geological Society of America Bulletin, v. 108, no. 12, p. 1515-1527.

Morgan, S.S. and Law, R.D., 1998, An overview of Paleozoic and Mesozoic structures developed in the central White-Inyo Range, eastern California: International Geology Review, v. 40, p. 245-256.

Morgan, S.S, Law, R.D., and Nyman, M.W., 1998, Laccolith-like emplacement model for the Papoose Flat Pluton based on porphyroblast-matrix analysis: Geological Society of America Bulletin, v. 110, no.1, p. 96-110.

Nokleberg, W.J., 1983, Wallrocks of the central Sierra Nevada batholith, California: a collage of accreted tectano-stratigraphic terranes: U. S. Geological Survey Professional Paper 1255, 28 p.

Passchier, C.W., 1988, Analysis of deformation paths in shear zones: Geologisches Rundschau, v. 77, p. 309-318.

Ramsay, J.G. and Graham, R.H., 1970, Strain variation in shear belts: Canadian Journal of Earth Sciences, v. 7, p. 786-813.

Reheis, M.C. and Dixon, T.H., 1996, Kinematics of the eastern California shear zone: evidence for slip transfer from Owens and Saline Valley fault zones to Fish Lake Valley fault zone: Geology, v. 24, p. 339-342.

Reheis, M.C. and Sawyer, T.L., 1997, Late Cenozoic history and slip rates of the Fish Lake Valley, Emigrant Peak, and Deep Springs fault zones, Nevada and California: Geological Society of America Bulletin, v. 109, p. 280-299.

Saint Blanquat, M., Law, R.D, Bouchez, J.L., and Morgan, S.S., 2001, Internal structure and emplacement of the Papoose Flat pluton; an integrated structural, petrographic, and magnetic susceptibility study: Geological Society of America Bulletin, v. 113, no. 8, p. 976-995.

Schweikert, R.A., 1981, Tectonic evolution of the Sierra Nevada Range, *in*, Ernst, W.G., ed., The geotectonic evolution of California: Englewood Cliffs, Prentice Hall, p. 87-130.

Simpson, C. and De Paor, D.G., 1993, Strain and kinematic analysis in general shear zones: Journal of Structural Geology, v. 15, p. 1-20.

Simpson, C. and De Paor, D.G., 1997, Practical analysis of general shear zones using porphyroclast hyperbolic distribution method: an example from the Scandinavian Caledonides, *in* Sengupta, S., ed., Evolution of geological structures in micro- to macro-scales, London, Chapman and Hall, p. 169-184.

Stern, T.W., Bateman, P.C., Morgan, B.A., Newell, M.F., and Peck, D.L., 1981, Isotopic U-Pb ages of zircons from the granitoids of the central Sierra Nevada, California: U. S. Geological Survey Professional Paper 1185, 17 p.

Stevens, C.H., Stone, P., Dunne, G.C., Greene, D.C., Walker, J.D., and Swanson, B.J., 1997, Paleozoic and Mesozoic evolution of east-central California: International Geology Review, v. 39, p. 788-829.

Stewart, J.H., 1980, Regional tilt patterns of late Cenozoic basin-range fault blocks, western United States: Geological Society of America Bulletin, v. 91, p. 460-464.

Stockli, D.F., Dumitru, T.A., McWilliams, M.O., and Farley, K.A., Cenozoic tectonic evolution of the White Mountains, California and Nevada: Geological Society of America Bulletin, v. 115 (in press).

Stockli, D.F., Farley, K.A., and Dumitru, T.A., 2000, Calibration of the apatite (U-Th)/He thermochronometer on an exhumed fault block, White Mountains, California: Geology, v. 28, no. 11, p. 983-986.

Tikoff, B. and Saint Blanquat, M., 1997, Transpressional shearing and strike-slip partitioning in the Late Cretaceous Sierra Nevada magmatic arc, California. Tectonics 16, 442-459.

Tikoff, B., and Greene, D.C., 1997. Stretching lineations in transpressional shear zones: an example from the Sierra Nevada batholith, California. Journal of Structural Geology 19, 29-39.

Tullis, J.A., Christie, J.M. and Griggs, D.T., 1973, Microstructures and preferred orientations of experimentally deformed quartzites: Geological Society of America Bulletin, v. 84, p. 297-314.

Vines, J.A., 1999. Emplacement of the Santa Rita Flat pluton and kinematic analysis of cross cutting shear zones, eastern California. Unpublished M.S. thesis, Blacksburg, Virginia Polytechnic Institute and State University, 89 p.

Wallis, S.R., 1992, Vorticity analysis in a metachert from the Sanbagawa Belt, SW Japan: Journal of Structural Geology, v. 14, p. 271-280.

Wallis, S.R., 1995, Vorticity analysis and recognition of ductile extension in the Sanbagawa Belt, SW Japan: Journal of Structural Geology, v. 17, no. 8, p. 1077-1093.

APPENDIX A

This appendix provides a complete listing in tabular form of all orientation of foliation and stretching lineation data collected for this study, together with a map on which the locations of the field stations where data was collected have been plotted (Map 2). It is intended to be used as a data archive so that the data collected during the course of this study will be available to future workers.

Table 2 lists all of the structural field data in its original format, and Table 3 lists all of the data after rotation as described in the thesis text. Most of the orientations listed for a given field station are an average of three or more measurements. A listing of "weak fabric" indicates that the fabric was to weak to measure confidently with the available outcrop exposure. A listing of no fabric indicates that there was no visible fabric in the outcrop. If there is no listing in either the foliation or lineation column, then there was no measurable foliation or lineation in that outcrop.

Table 2: Table showing orientations of foliation and stretching lineations collected from the northern half of the White Mountain shear zone. The data is listed by field station, and the locations of the field stations are plotted on Map 2.

Field Station	Strike Fol.	Dip Fol.	Trend Lin.	Plunge Lin.
008	340	61-W		
009	324	74-W	146	08
010	329	46-E	356	24
011	302	76-S	287	46
013	281	47-S		
021	345	73-W	342	12
022	315	75-W	306	28
024	308	51-S		
025	311	59-S		
026	340	56-W	328	17
027	337	49-W	317	22
032	006	78-E	010	19
033	000	83-E	009	18
034	001	86-W		
035	350	74-W	348	07
036	344	75-E	352	23
037	000	73-E	006	18
038	316	69-W		
039	314	70-S	140	15
040	327	74-W	149	08
041	317	54-W	315	03
042	299	59-W	292	11
043	320	55-W		
044	314	50-W	309	07
045	319	47-W	149	10
046	314	44-W	141	09
047	312	49-W	301	11
048	314	52-W	137	04
049	289	64-S		
050	333	65-W	330	07
052	277	59-S		
053	306	52-W		
054	278	61-W		
055	296	71-W		
056	285	45-W		
057	323	70-W		
058	333	77-W		
059	309	66-W		
060	005	62-W		
061	004	60-W		
062	359	55-W		
063	003	49-W	342	23
064	007	55-W		
065	023	45-W	326	40
066	011	47-W	355	16
067	017	40-W	002	12

Field Station	Strike Fol.	Dip Fol.	Trend Lin.	Plunge Lin.
068	315	73-W		
069	342	65-W		
070	358	44-W	338	18
071	006	67-W	356	22
072	000	60-W		
073	Brecciated			
074	Brecciated			
075	050	50-W		
076	053	54-W	034	24
077	055	48-W		
078	053	34-W	351	30
079	300	72-S	293	21
080	326	66-W	316	20
081	310	62-S		
082	314	52-S	298	15
083	288	55-S	117	14
084	303	79-S		
085	296	73-S		
086	304	53-S	135	15
087	298	64-S	144	17
088			308	21
089	281	68-S		
090	300	62-S	291	15
091	313	75-S		
092	299	63-S		
093	287	70-S	280	18
094	288	63-S		
095	283	74-S		
096	033	75-W	022	36
097	038	70-W	020	39
098	040	75-W	026	38
099	036	71-W	025	29
100	039	84-W	035	33
101	022	56-W		
102	038	73-W		
103	034	63-W	018	29
104	022	67-W	008	30
105	014	50-W	347	28
106	016	51-W	345	31
107	013	56-W	341	38
108	016	44-W	356	18
109	285	32-S		
110	025	55-W		
111	027	34-W		
112	Weak	Fabric		
113	Weak	Fabric		
114	No	Visible	Fabric	
115	010	51-W		
116	054	35-W	003	28
117	032	20-W		
130	313	73-W		
131	318	66-W		

Field Station	Strike Fol.	Dip Fol.	Trend Lin.	Plunge Lin.
132	304	51-S		
133	313	61-S		
134	No	Visible	Fabric	
135	326	90	326	57
136	307	44-S		
137	328	45-W	309	18
138	No	Visible	Fabric	
139	329	49-W	318	12
140	No	Visible	Fabric	
141	No	Visible	Fabric	
142	299	59-S		
143	No	Visible	Fabric	
144	335	79-W		
145	316	84-W		
146	085	64-S		
147	332	75-S	326	21
148	277	62-S		
149	293	67-S		
150	320	78-W	315	22
151	303	63-S		
152	274	48-S		
153	274	64-S	109	28
154	290	72-S		
155	350	89-W		
156	322	73-W	290	46
157	320	64-W		
158	305	60-W	271	44
159	013	53-E	039	30
160	065	87-N	060	59
161	337	89-W	336	43
162	Not	in	Place	
163	332	45-E		
164	Not	in	Place	
165	003	42-W	349	12
166	351	59-E	018	19
167	027	68-W	011	33
170	331	53-W	255	52
174	068	44-N	338	44
	062	54-N	012	46
175	050	47-N		
176	035	43-W	025	09
177	032	59-W	341	52
178	No	Visible	Fabric	
179	043	52-W	012	33
180	No	Visible	Fabric	
181	347	77-W	339	33
182	033	70-E	040	13
183	012	58-W	012	01
184	026	65-W	024	03
185	029	80-E		
186	021	89-E		
187	010	54-W	002	10

Field Station	Strike Fol.	Dip Fol.	Trend Lin.	Plunge Lin.
188	019	54-W	004	19
189	024	88-E	025	07
190	019	80-E	023	23
191	No	Visible	Fabric	
192	No	Visible	Fabric	
193	338	41-W	278	37
194	No	Visible	Fabric	
195	353	78-W		
196	355	79-W		
197	003	84-E	176	54
198	351	65-W	234	63
199	324	50-W	234	49
200	310	55-S	248	52
201	328	47-W	262	44
202	312	62-S	286	39

Table 3: Table showing orientations of foliation and stretching lineations collected from the northern half of the White Mountain shear zone that have been rotated 25° counterclockwise about a horizontal line trending towards 355°. The data is listed by field station, and the locations of the field stations are plotted on Map 2.

Field Station	Strike Fol.	Dip Fol.	Trend Lin.	Plunge Lin.
008	342	85-W		
009	324	84-E	325	05
010	308	36-N	007	21
011	316	87-E	134	27
013	298	58-S		
021	345	83-E	349	16
022	316	85-E	320	45
024	318	70-W		
025	317	78-W		
026	343	80-W	337	26
027	341	73-W	329	35
032	008	54-E	016	11
033	008	58-E	009	11
034	001	69-E		
035	350	81-E	352	09
036	341	51-E	003	22
037	001	48-E	012	12
038	318	89-W		
039	317	89-W	317	01
040	328	86-E	328	03
041	325	74-W	321	19
042	308	74-S	297	31
043	326	76-W		
044	323	70-W	312	24
045	327	68-W	327	01
046	325	64-W	321	05
047	322	68-W	308	30
048	322	68-W	318	11
049	297	76-W		
051	331	76-W	331	00
052	289	67-W		
053	294	61-W		
054	289	69-W		
055	300	85-W		
056	303	58-W		
057	325	88-E		
058	333	79-E		
059	319	86-W		
060	004	87-W		
061	003	85-W		

Field Station	Strike Fol.	Dip Fol.	Trend Lin.	Plunge Lin.
068	317	87-E		
069	344	89-W		
070	357	70-W	348	24
071	005	89-E	006	20
072	359	85-W		
073	Brecciated			
074	Brecciated			
075	038	68-W		
076	042	70-W	039	07
077	042	63-W		
078	032	52-W	005	29
079	304	87-S	302	43
080	329	88-W	327	34
081	316	81-W		
082	322	72-W	305	35
083	300	68-S	297	06
084	304	85-N		
085	300	86-S		
086	314	70-W	313	01
087	305	79-S	126	04
088			319	38
089	289	77-S		
090	308	78-S	297	36
091	314	85-E		
092	306	79-S		
093	293	81-S	291	40
094	297	74-S		
095	288	83-S		
096	032	85-E	035	22
097	035	89-W	034	26
098	039	86-E	040	23
099	034	89-E	034	15
100	040	78-E	043	15
101	018	79-W		
102	037	88-E		
103	030	83-W	028	17
104	020	89-W	020	22
105	010	74-W	001	29
106	012	75-W	003	32
107	010	80-W	002	40
108	011	68-W	004	16
109	311	46-S		
110	020	77-W		
111	016	56-W		
112	Weak	Fabric		
113	Weak	Fabric		

Field Station	Strike Fol.	Dip Fol.	Trend Lin.	Plunge Lin.
132	316	68-W		
133	319	81-W		
134	No	Visible	Fabric	
135	324	68-E		
136	320	64-W		
137	334	68-W		
138	No	Visible	Fabric	
139	330	71-W	323	21
140	No	Visible	Fabric	
141	No	Visible	Fabric	
142	308	74-W		
143	No	Visible	Fabric	
144	335	77-E		
145	315	78-E		
146	285	56-S		
147	334	82-E	337	31
148	288	70-S		
149	299	80-S		
150	320	81-E	327	36
151	310	78-S		
152	293	56-S		
153	284	70-S	106	06
154	294	84-S		
155	350	66-E		
156	323	86-E	332	62
157	329	85-W		
158	313	77-W	275	69
159	025	30-E	046	12
160	066	86-S	070	36
161	334	68-E	001	46
162	Not	in	Place	
163	311	25-N		
164	Not	in	Place	
165	002	67-W	355	14
166	349	34-E	010	14
167	025	89-W	024	23
170	336	76-W	246	76
174	049	56-N	003	46
	050	66-N	032	34
175	037	64-W		
176	025	63-W	206	03
177	027	80-W	013	51
178	No	Visible	Fabric	
179	033	70-W	024	23
180	No	Visible	Fabric	
181	347	78-E	357	36

Field Station	Strike Fol.	Dip Fol.	Trend Lin.	Plunge Lin.
188	015	87-W	013	14
189	026	68-E	206	06
190	023	57-E	024	01
191	No	Visible	Fabric	
192	No	Visible	Fabric	
193	343	66-W	286	61
194	No	Visible	Fabric	
195	353	77-E		
196	355	76-E		
197	004	60-E	146	47
198	352	90	172	78
199	331	72	206	67
200	318	74-W	228	74
201	334	70-W	258	69
202	318	81-W		

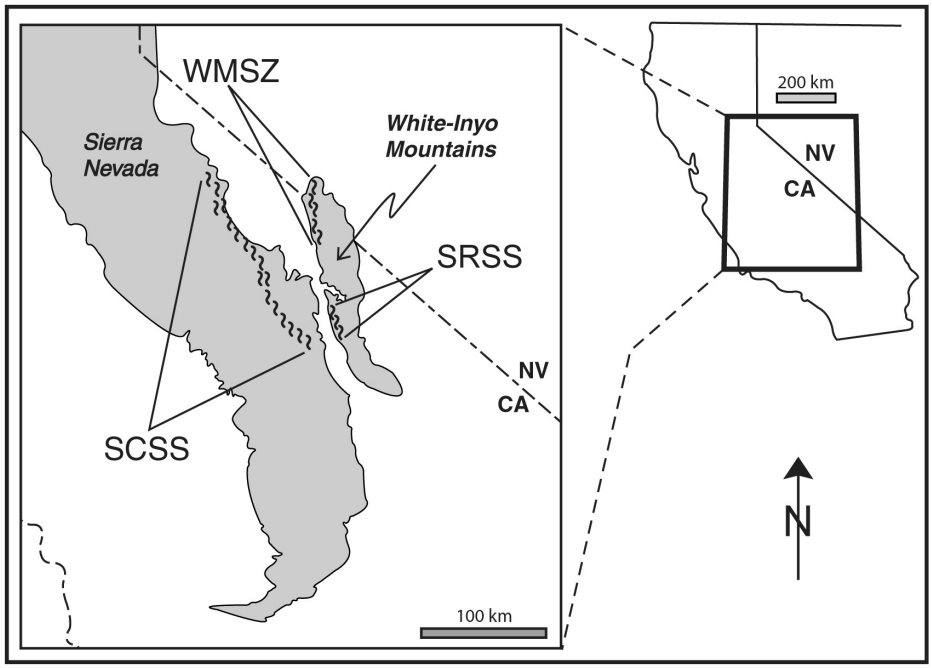

Figure 1: Map showing locations of the White Mountain shear zone (WMSZ), Sierra Crest shear system (SCSS) and Santa Rita shear system (SRSS) relative to the Sierra Nevada and White-Inyo Range in eastern California and Nevada. Adapted from Greene and Schweikert, 1995; and Stevens et. al., 1997.

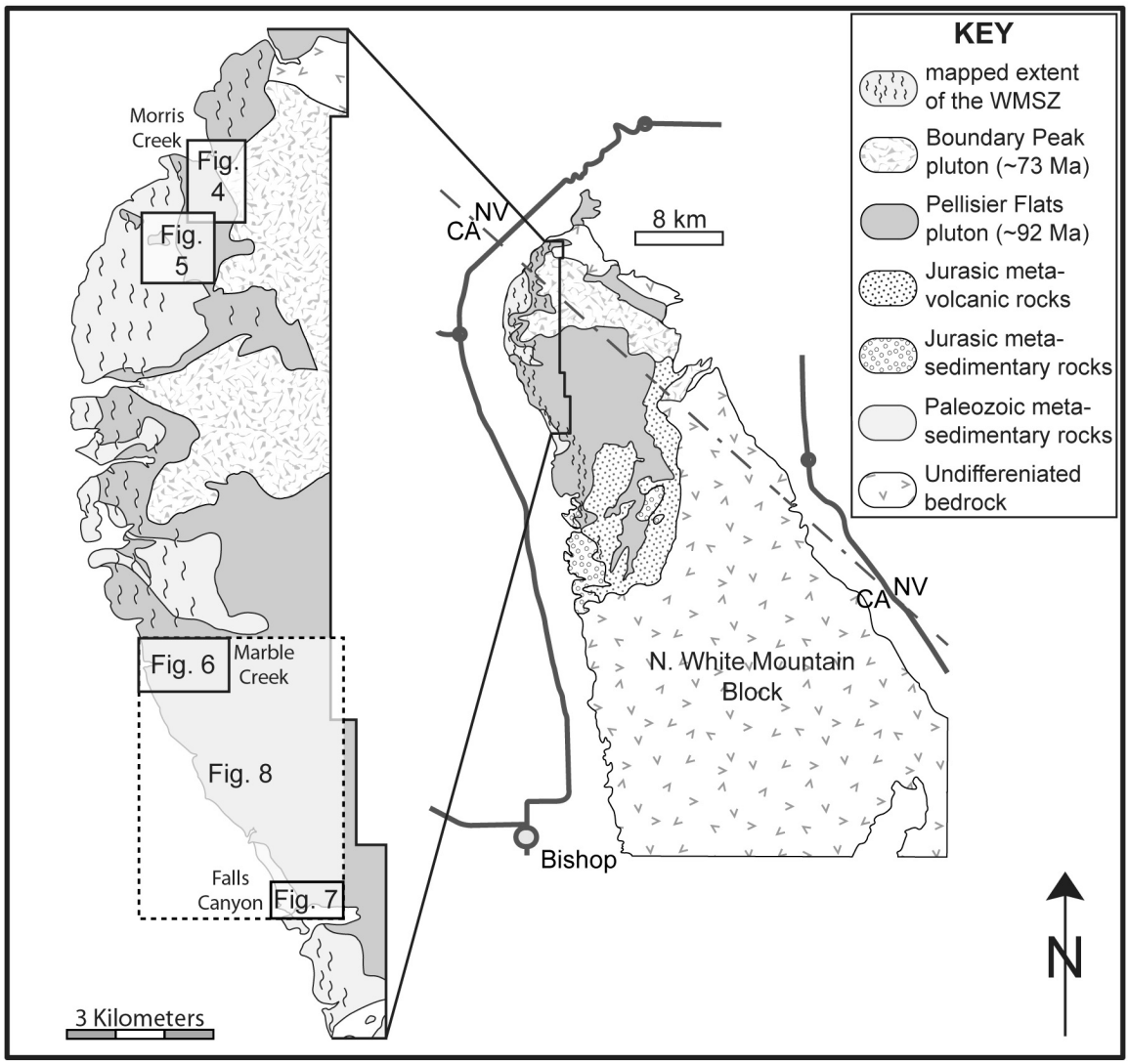

Figure 2: Map showing location of the field area for this study (left hand side) and the general geology of the northern White Mountains adjacent to the WMSZ (right hand side). Adapted from Crowder et. al., 1972; Crowder and Sheridan, 1972; and Crowder and Ross, 1973.

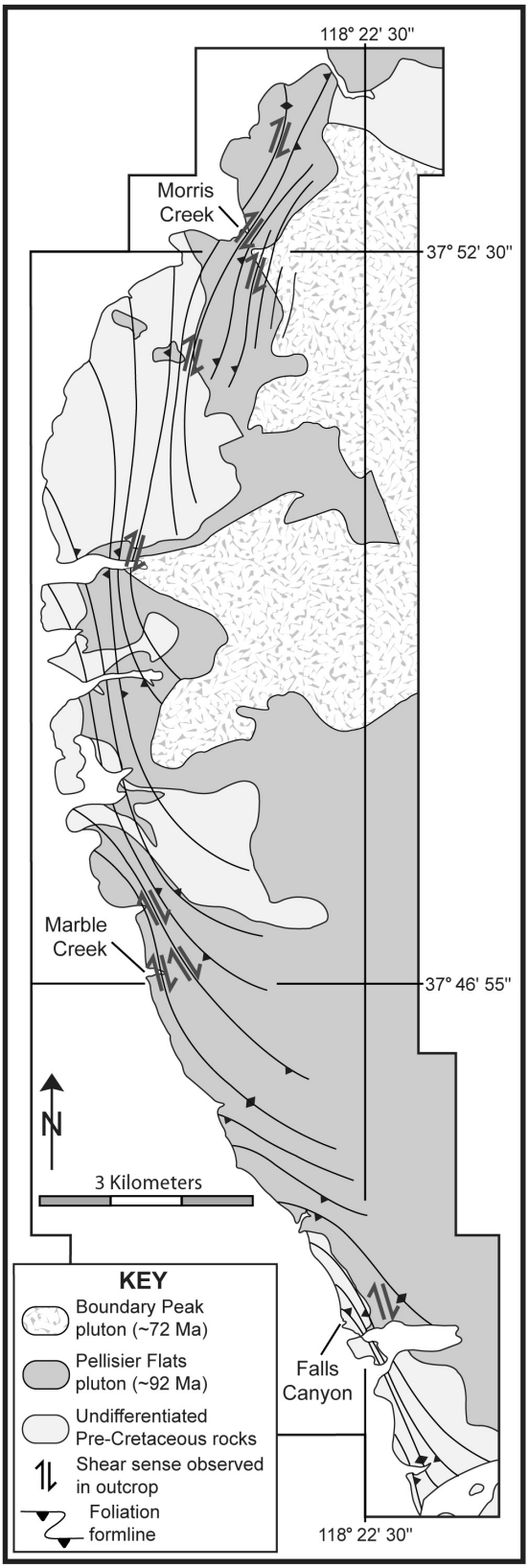

Figure 3: Map of the study area showing generalized foliation form-lines for the northern half of the WMSZ and locations where dextral S-C fabrics were observed in outcrop. Lithologic contacts are modified from Crowder et. al., 1972; and Crowder and Sheridan, 1972.

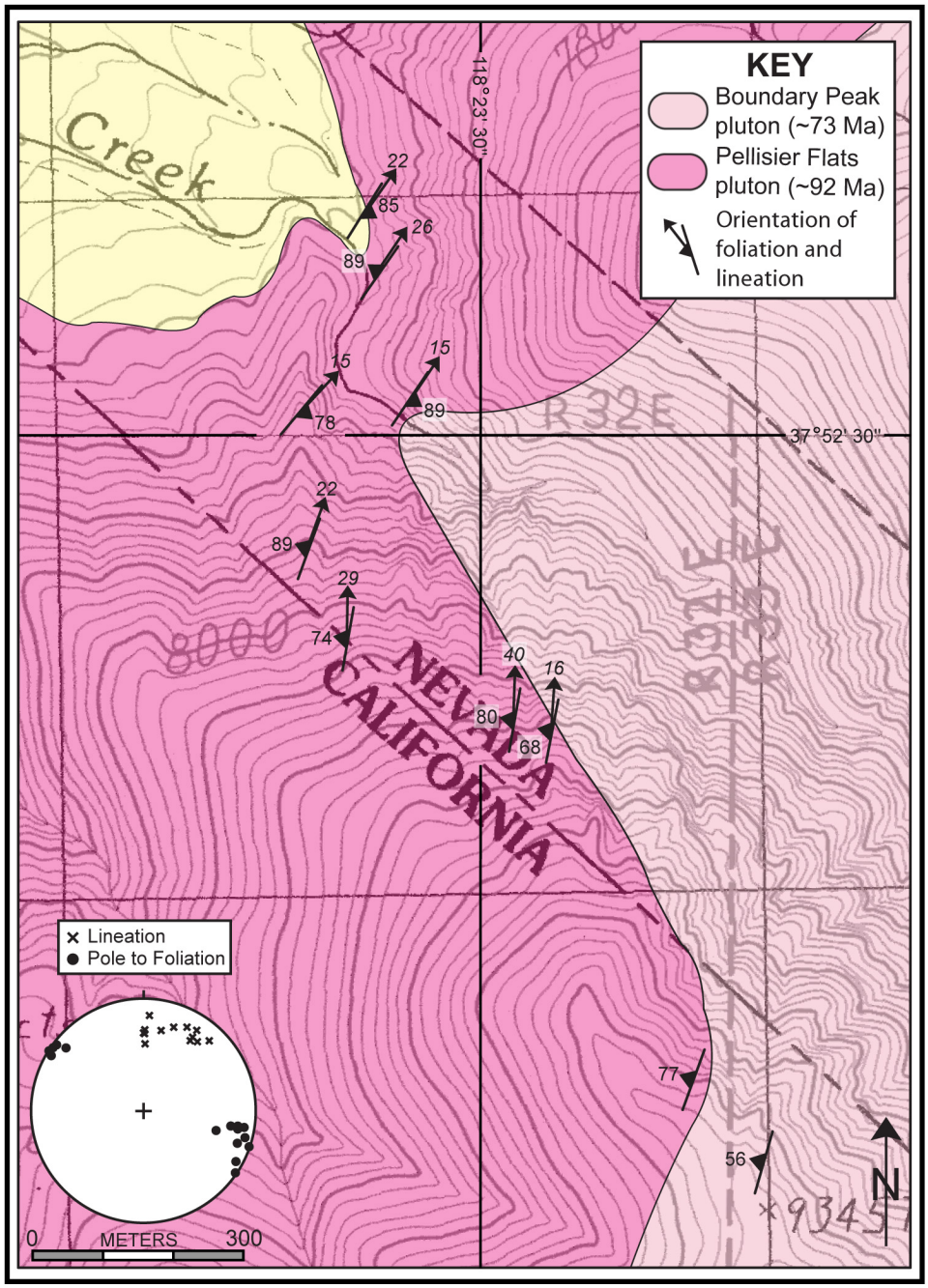

Figure 4: Map showing representative orientations of foliation and stretching lineations within the WMSZ in the Morris Creek area. Foliation and lineation data for this transect is summarized on an equal angle stereographic projection. The data has been rotated as discussed in the text. The location of the map area is shown in Fig. 2. Lithologic contacts are modified from Crowder et. al., 1972.

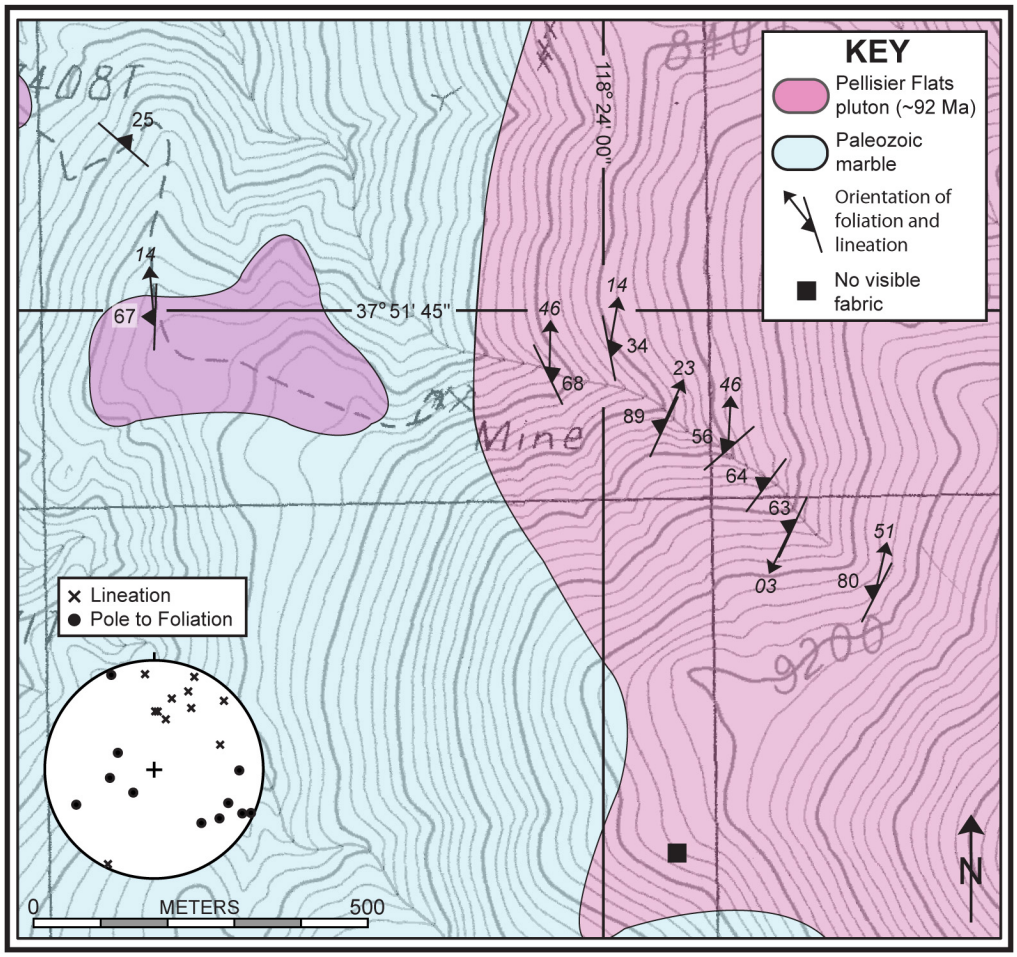

Figure 5: Map showing representative orientations of foliation and stretching lineations within the WMSZ south of Morris Creek. Note alternating steeply plunging and shallowly plunging stretching lineations. Foliation and lineation data for this transect is summarized on an equal angle stereographic projection. The data has been rotated as discussed in the text. The location of the map area is shown in Fig. 2. Lithologic contacts are modified from Crowder et. al., 1972.

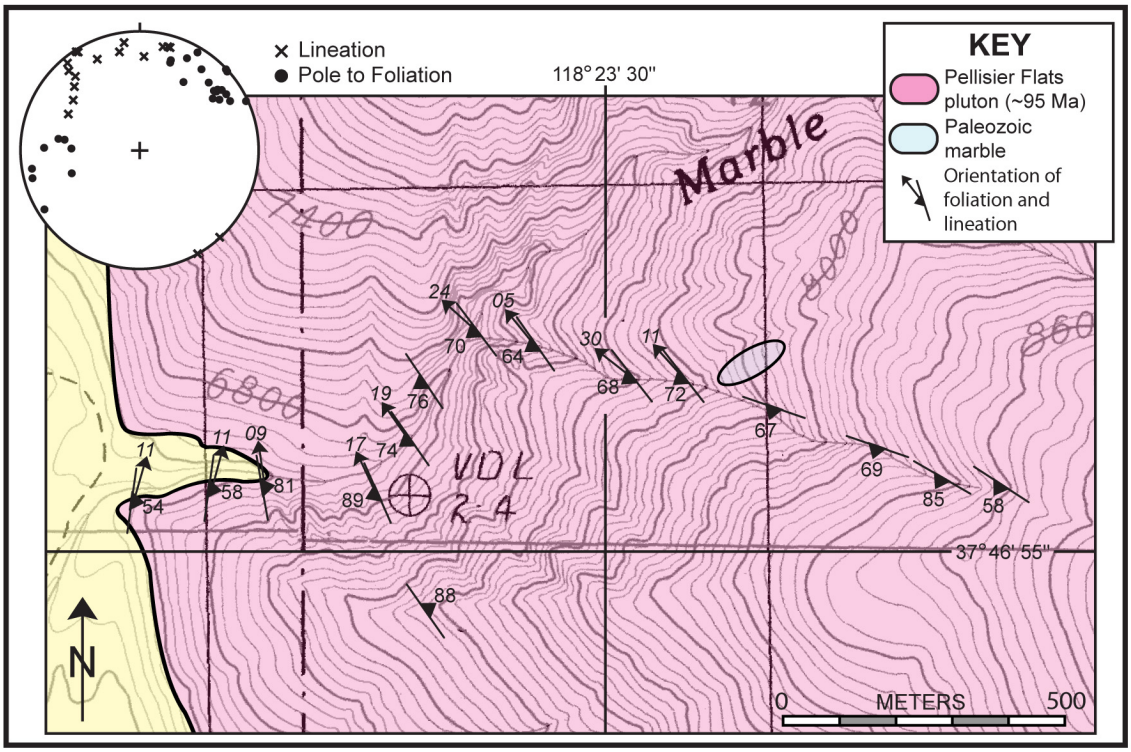

Figure 6: Map showing representative orientations of foliation and stretching lineations within the WMSZ in the area of Marble Creek. Note the swing in the strike of foliation from ~N-S near the range front to ~NW near the shear zone margins. Foliation and lineation data for this transect is summarized on an equal angle stereographic projection inset in the map. The data has been rotated as discussed in the text. The location of the map area is shown in Fig. 2. Lithologic contacts are modified from Crowder et. al., 1972.

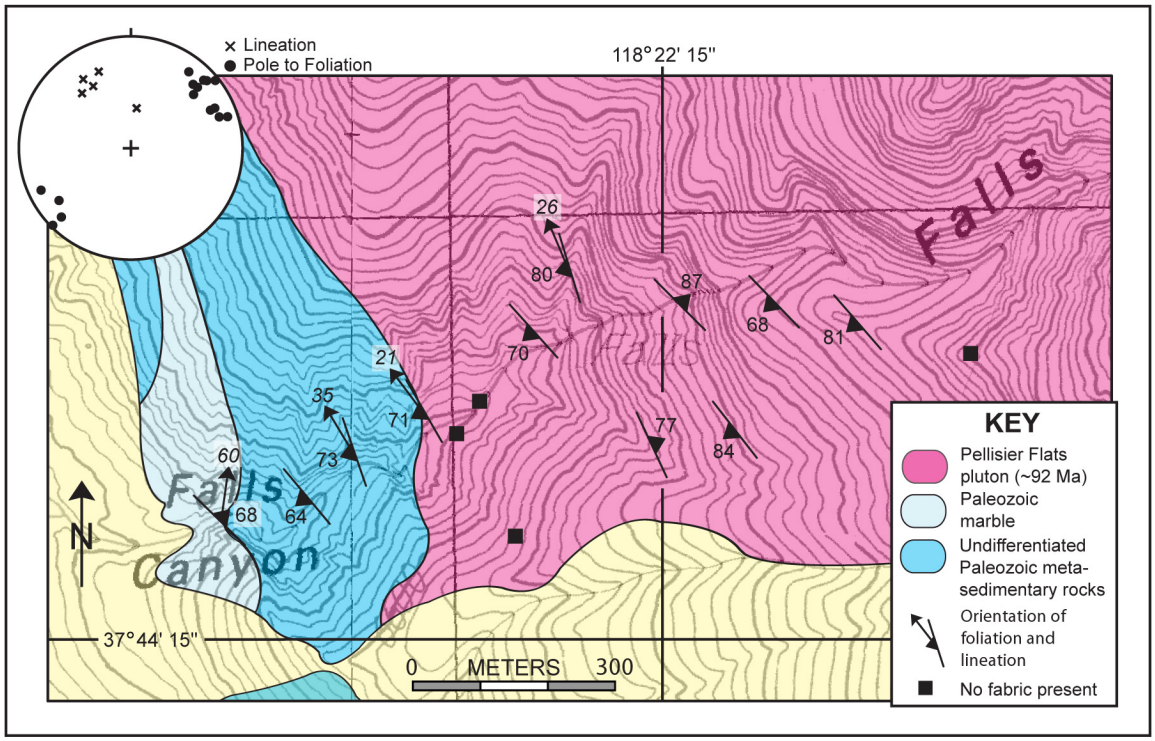

Figure 7: Map showing representative orientations of foliation and stretching lineations within the WMSZ in the area of Falls Canyon. Foliation and lineation data for this transect is summarized on an equal angle stereographic projection inset in the map. The data has been rotated as discussed in the text. The location of the map area is shown in Fig. 2. Lithologic contacts are modified from Crowder and Sheridan, 1972

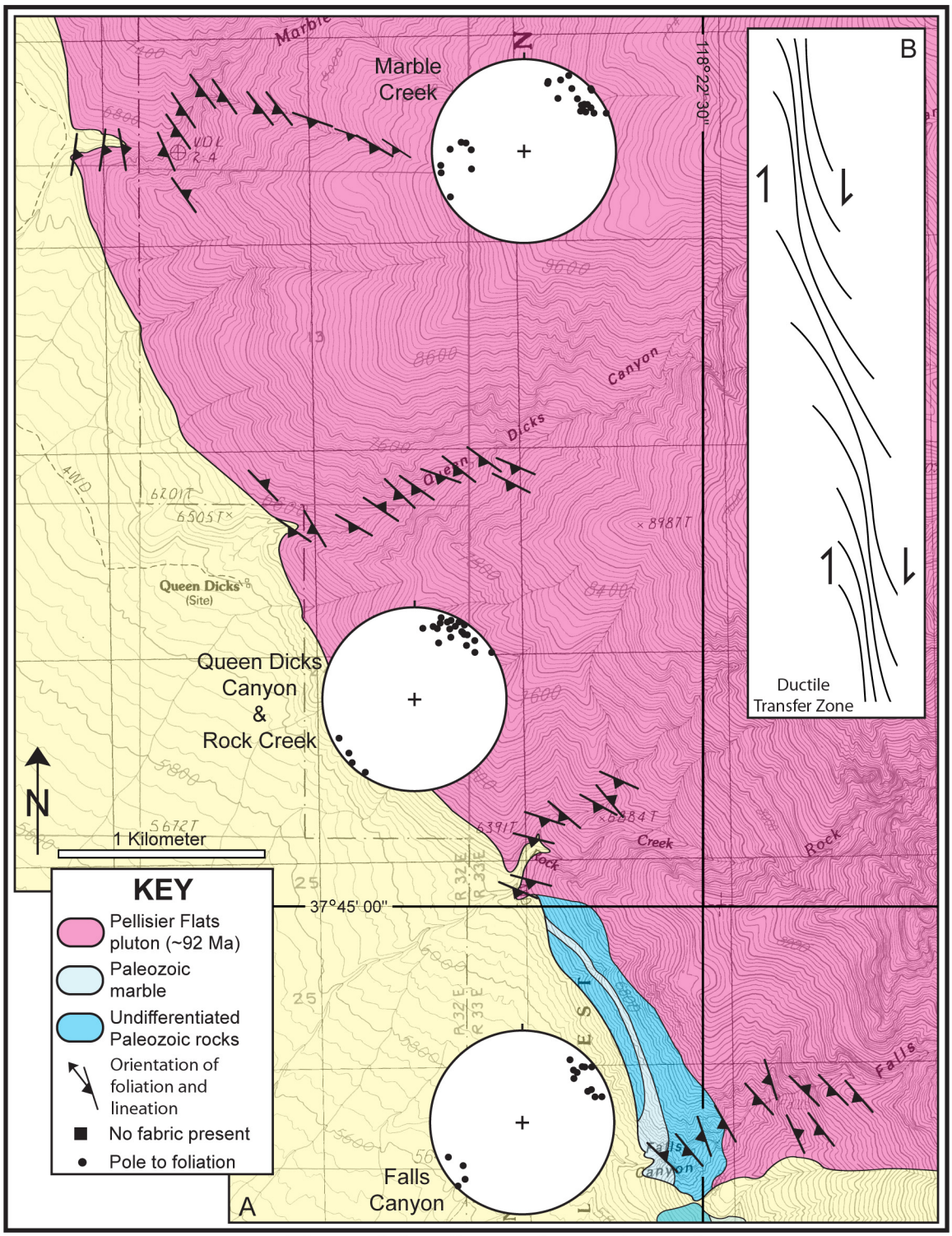

Figure 8 (caption on the next page)

Figure 8: A) Map showing representative orientations of foliation for a proposed left stepping transfer zone between discrete NNE and NNW striking segments of the WMSZ between Marble Creek and Falls Canyon. Equal angle stereographic projections summarize all of the foliation data for the Marble Creek area (top), the proposed transfer zone (center) and the Falls Canyon area (bottom). The data has been rotated as discussed in the text. The location of the map area is shown in Fig. 2. Lithologic contacts are modified from Crowder et al., 1972; and Crowder and Sheridan, 1972. B) Diagram illustrating the concept of a left stepping transfer zone between segments of a ductile shear zone.

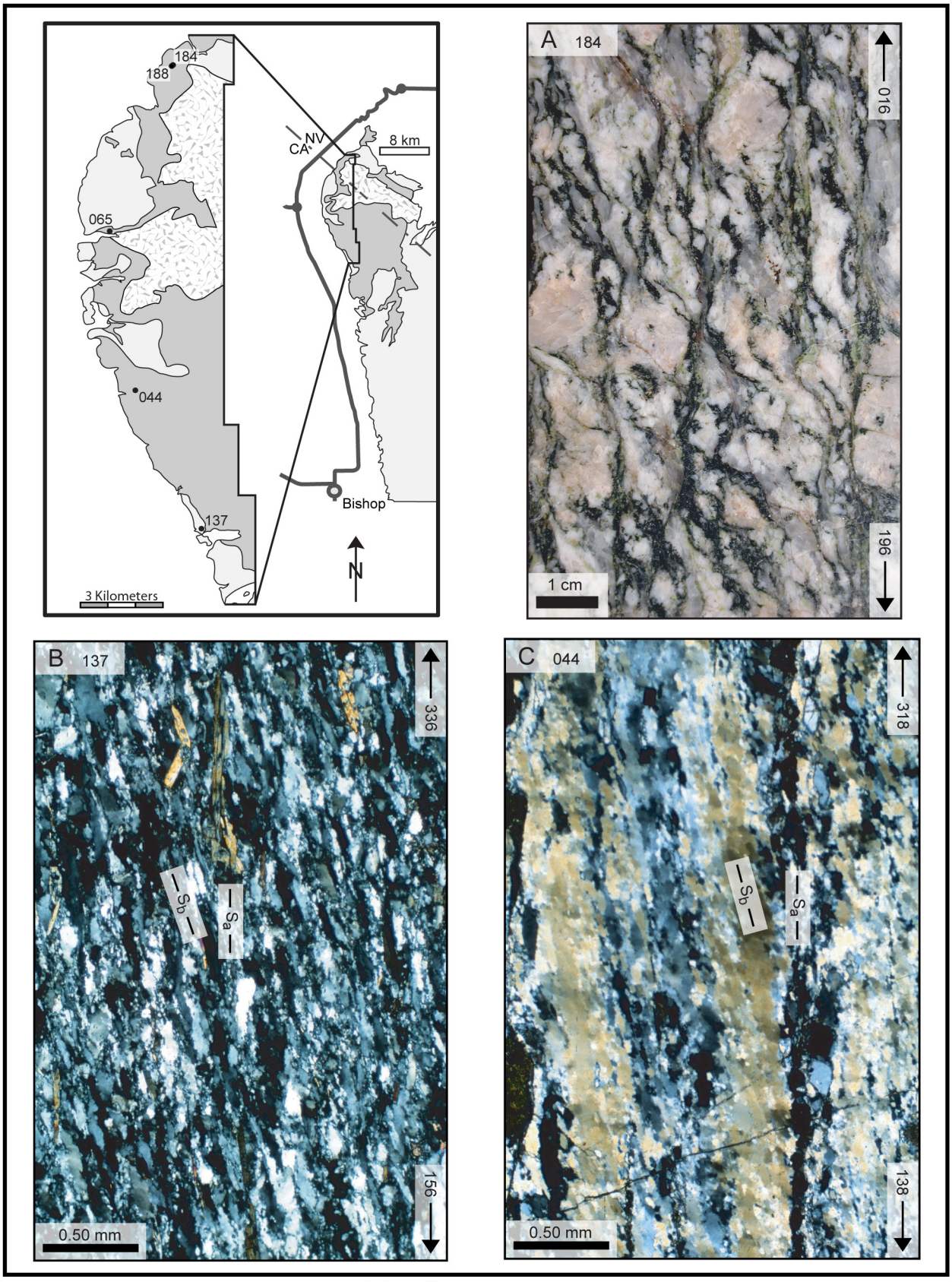

Figure 9 (continued on the next page)

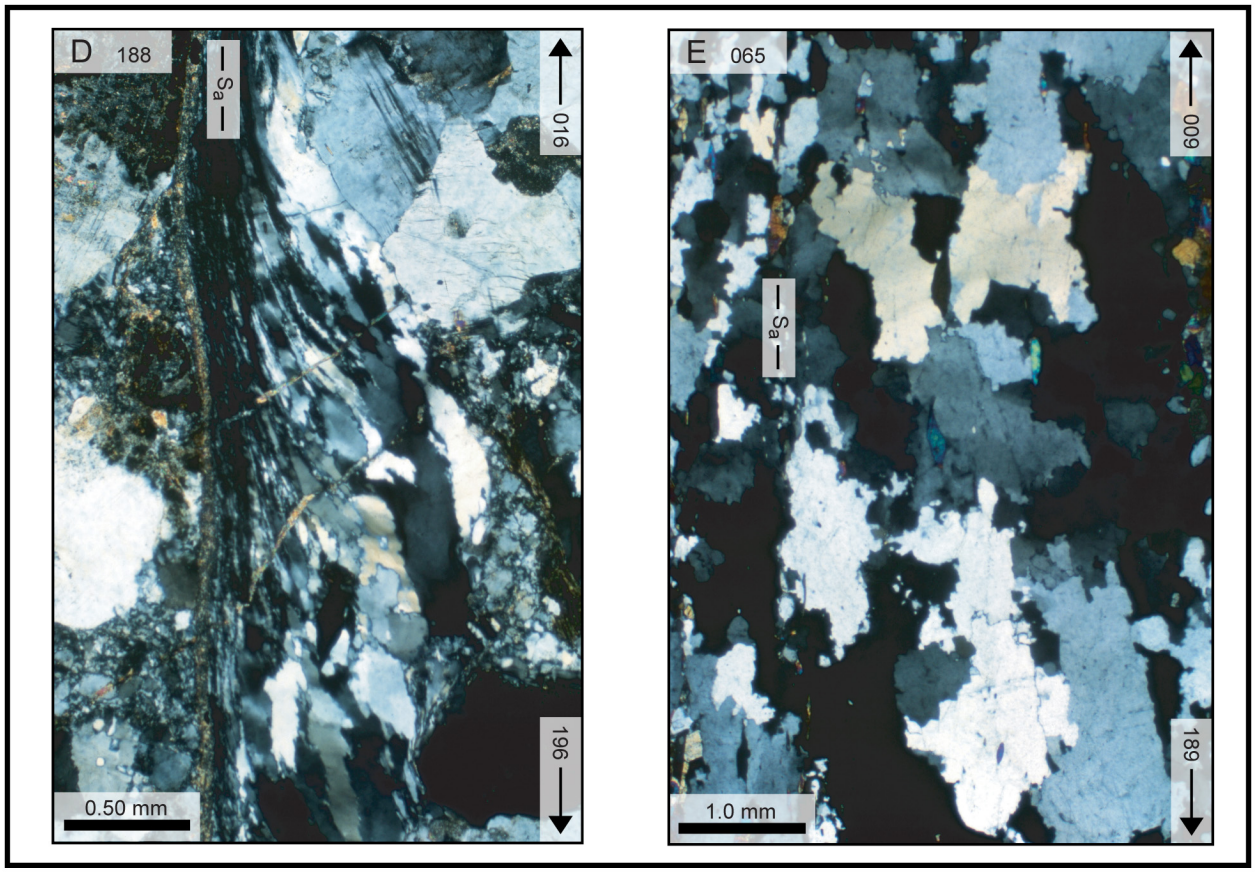

Figure 9: A) Dextral type I S-C fabrics on a cut face of an oriented hand sample. B) regime II quartz recrystallization (Hirth and Tullis 1992) in a dextral type II S-C mylonite from Falls Canyon. C) Regime II quartz recrystallization in a dextral type II S-C mylonite from Marble Creek. D) Transition from regime II and III quartz recrystallization between relatively high strain C-surface and relatively low strain S-surface. E) Regime III quartz recrystallization from a sheared quartzite xenolith hosted within the deformed Pellisier Flats pluton. All views are perpendicular to foliation and parallel to lineation. A, C and D are from subhorizontally lineated samples, and B and E are from steeply lineated samples. Sample numbers are in the upper left hand corners of the micrographs.

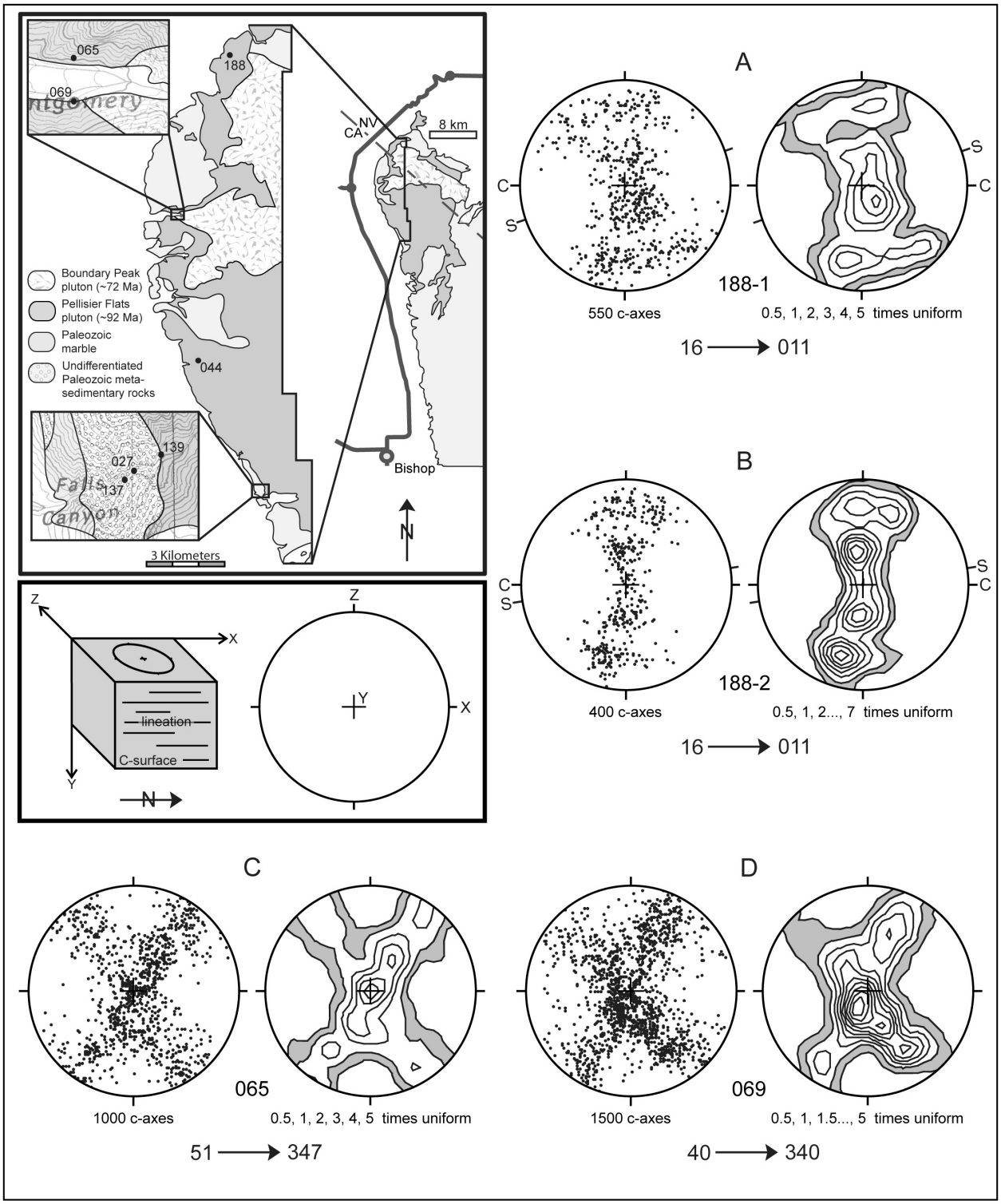

Figure 10 (continued on the next page)

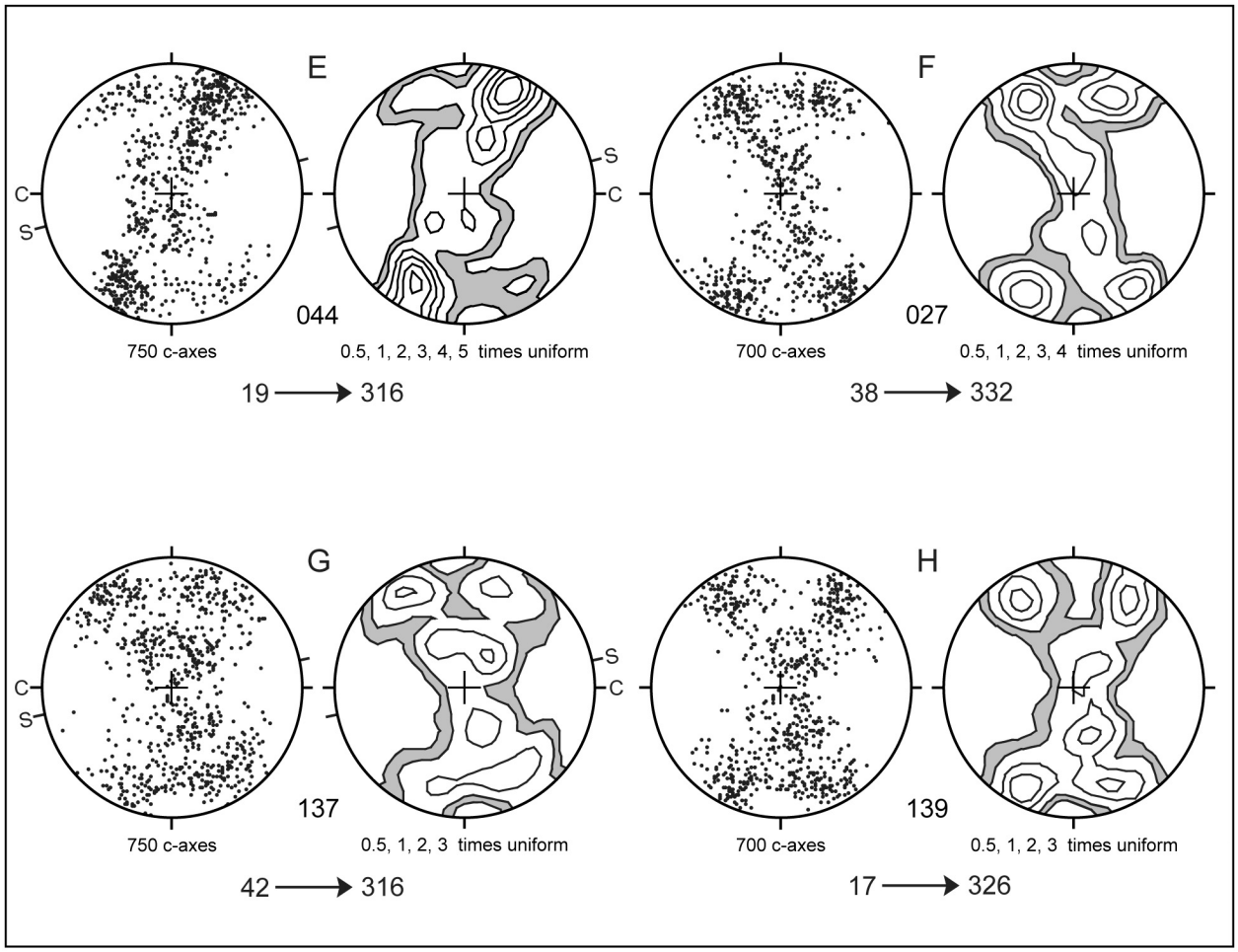

Figure 10: Quartz c-axis fabrics from the northern half of WMSZ. A) and B) are from different domains of the same sample from the Pellisier Flats Pluton, with A) containing both regime II and III recrystallization and B) being dominated by regime II recrystallization (see text for explanation). C) and D) are form metasedimentary xenoliths from within the Pellisier Flats pluton. E) is from Marble Creek and was collected from a sheared quartz vein within the Pellisier Flats pluton. F-H) are from Falls Canyon and were collected from sheared quartzose metamorphic rocks. All projections are equal area lower hemisphere oriented perpendicular to the steeply dipping foliation and parallel to the stretching lineation. Orientations of S-surfaces have been marked for samples where S-C relations were observed. Trend and plunge of the stretching lineation is given below the fabric plots.

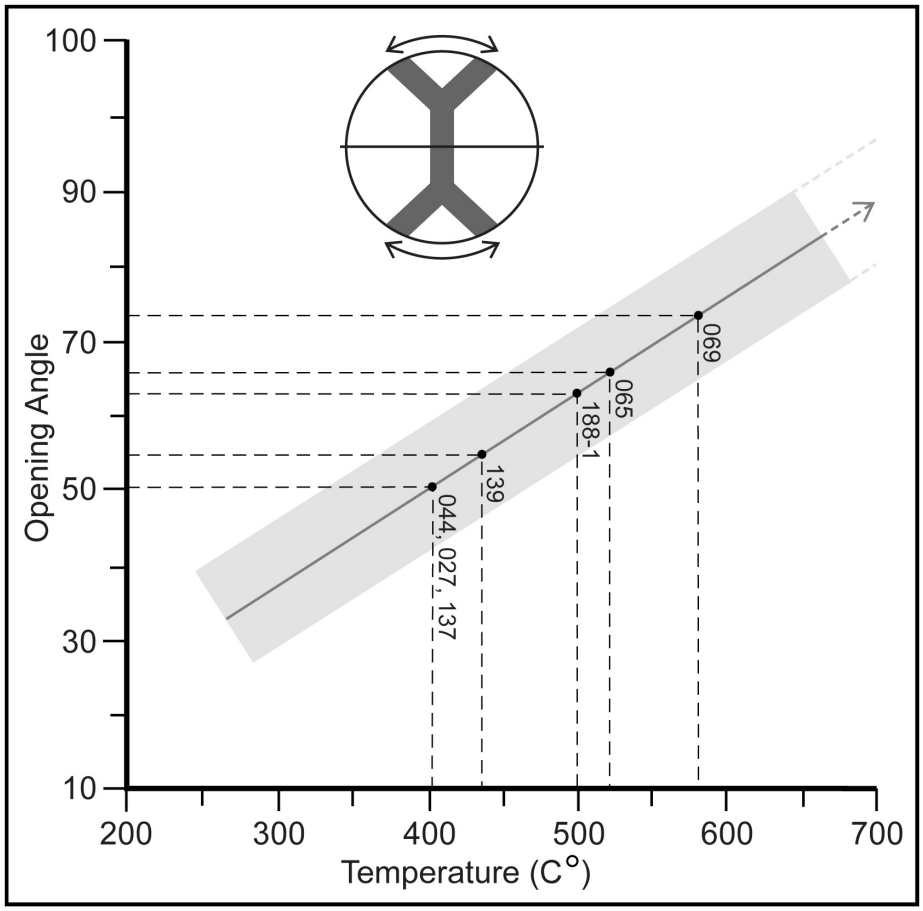

Figure 11: Geothermometer based on the opening angle of quartz c-axis fabrics; adapted from Kruhl (1998). Opening angles of c-axis fabrics from the WMSZ are plotted. Samples 069 and 065 were collected from sheared quartzites from xenoliths hosted within the Pellisier Flats pluton. Sample188 was collected from the Pellisier Flats pluton. Sample 044 was collected from a sheared quartz vein in the Pellisier Flats pluton. Samples 139, 137 and 027 were collected from sheared quartzose metamorphic rocks. See Figure 10 for sample locations.

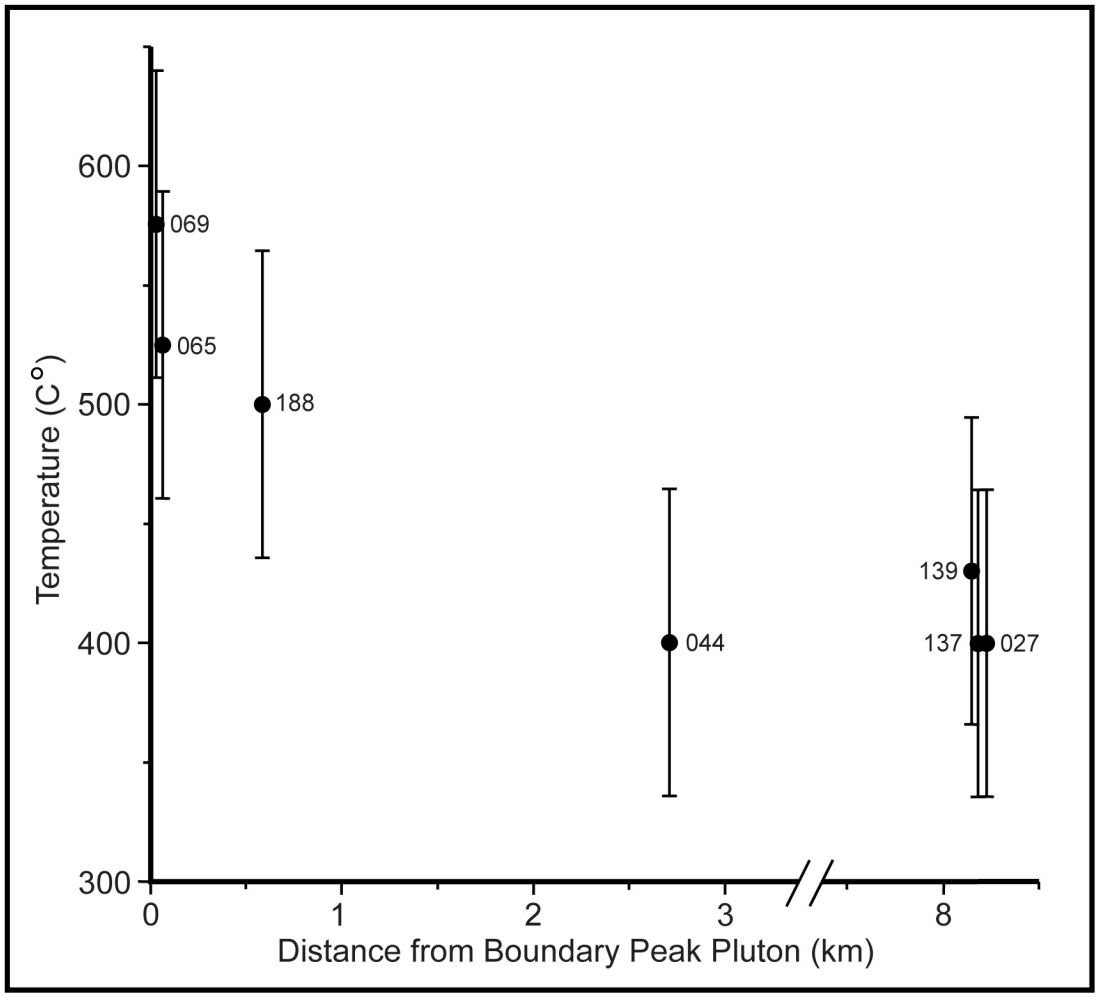

Figure 12: Plot of deformation temperatures, estimated from the Kruhl (1998) geothermometer, vs. horizontal distance from the Boundary Peak pluton. See Figure 10 for sample locations and Figure 11 for lithologies.